

## Integrating HER and OER Active Sites in a Two-Dimensional Covalent Terephthalaldehyde-based Framework for Metal-Free Photocatalytic Overall Water Splitting

Xin Wang<sup>a</sup>, Jiao Chen<sup>a\*</sup>, Xinyong Cai<sup>b</sup>, Tian Tang<sup>a</sup>, Chunsheng Guo<sup>a</sup>, Yuxiang Ni<sup>a</sup>, Yuanzheng Chen<sup>a</sup>, Hongyan Wang<sup>a\*</sup>

<sup>a</sup> School of Physical Science and Technology, Southwest Jiaotong University, Chengdu 610031, China.

<sup>b</sup> School of Materials Science and Engineering, Xihua University, Chengdu 610039, China.

\*E-mail: [j.chen.swjtu@outlook.com](mailto:j.chen.swjtu@outlook.com) (J. C.) and [hongyanw@swjtu.edu.cn](mailto:hongyanw@swjtu.edu.cn) (H. W.)

### Table of Contents for Supporting Information

Free energy change of HER and OER on linkages and building units .....	1
Proposed five-step synthetic route to TTTP .....	2
Computational details for Poisson's ratio and The Young's modulus .....	3
Comparison of band structure calculated in vacuum and aqueous solution .....	3
Calculated $\eta_{STH}$ as a function of QE for 2D CTF and various COFs .....	4
Adsorption of H <sub>2</sub> O molecules on the surfaces of 2D CTF .....	5
COHP/ICOHP analysis of key adsorbate-substrate bonds .....	7
Computational details for carrier mobility .....	8
Computational details for free energy change and formation energy .....	8
References .....	11

## Free energy change of HER and OER on linkages and building units

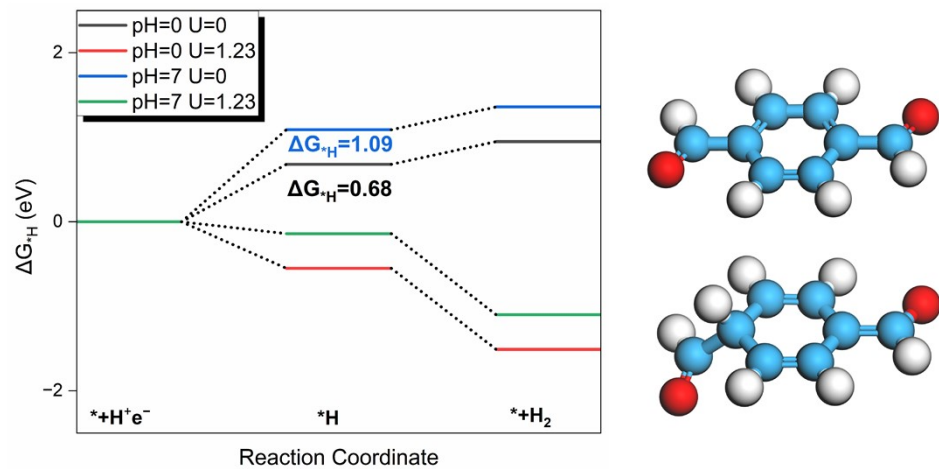


**Fig. S1.** Free energy change of HER process on TPA.

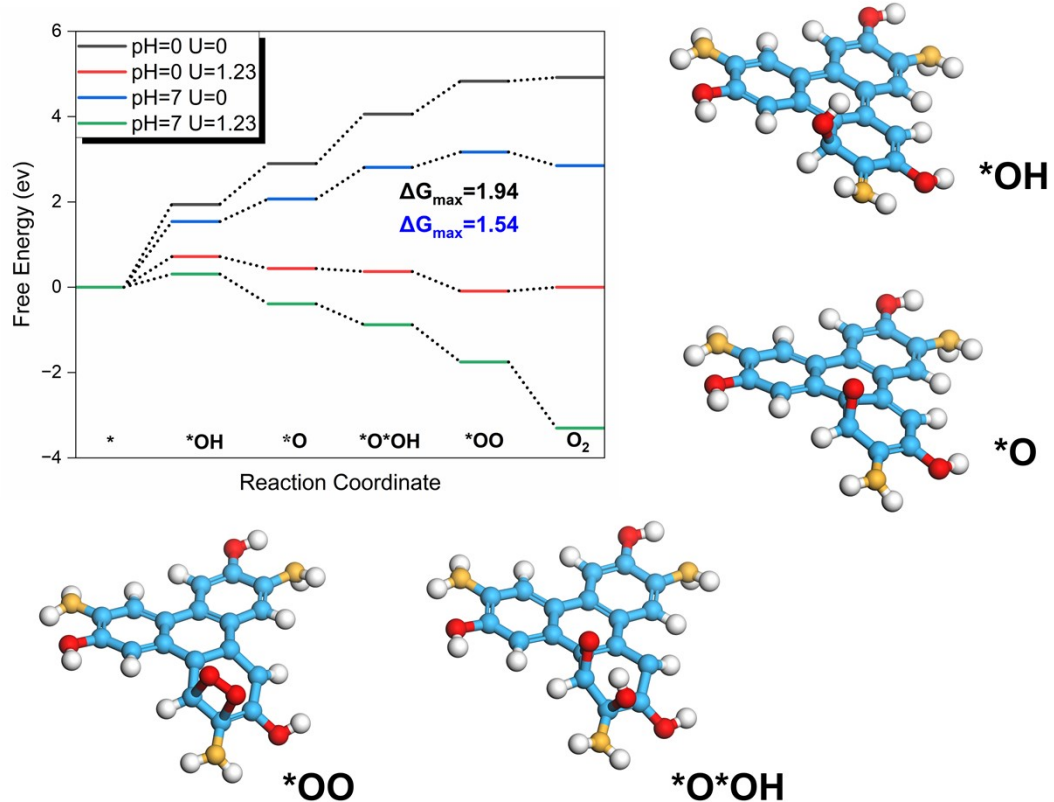


**Fig. S2.** Free energy change of OER process on TTPP.

## Proposed five-step synthetic route to TTTP

Based on previously reported synthetic mechanisms and methodologies, a five-step synthetic route to TTTP is proposed, as illustrated in Fig. S3†. The HHTP(I) can first undergo exhaustive O-alkylation to its poly-alkoxy derivatives 2,3,6,7,10,11-hexamethyltriphenyl (HMTP, II), as documented in the literature [RSC Advances 2014, 4, 38281-38292]<sup>6</sup>, providing a direct precedent for O-methylation under standard Williamson conditions using  $(\text{CH}_3)_2\text{SO}_4/\text{K}_2\text{CO}_3$ . This is followed by a controlled  $\text{BBr}_3$ -mediated demethylation (low equivalents,  $-78$  to  $0$  °C) to selectively expose three hydroxyl groups to yield III, as documented in the literature [Green Chemistry, 2023, 25(24), 10117-10143], which highlights how controlled equivalents, temperature, and electronic effects enable selective O-demethylation. The three exposed hydroxyls can then be triflated ( $-\text{OH} \rightarrow -\text{OTf}$ ) with  $\text{Tf}_2\text{O}$  and pyridine to afford the 3 $\times$ OTf intermediate (IV), as documented in the literature [Org. Synth. 2002, 79, 43]<sup>8</sup> and [Chem. Sci. 2022, 13, 2663–2672]<sup>9</sup>. The subsequent Pd-catalyzed amination of aryl triflates ( $-\text{OTf} \rightarrow -\text{NH}_2$ ) to yield V, as documented in the literature [Chayasith Uttamapinant Chembiochem. 2011]<sup>10</sup> and [Chem. Rev. 2016, 116, 12564]<sup>11</sup>. Finally, a full-equivalent  $\text{BBr}_3$  demethylation restores the remaining hydroxyl groups, yielding the target TTTP, as documented in the literature [Organic Syntheses, Coll. Vol. 5, p.412 (1973); Vol. 49, p.50 (1969) ]<sup>12</sup>. Each of these steps is supported by well-established literature precedents, strongly supporting the synthetic feasibility of TTTP.

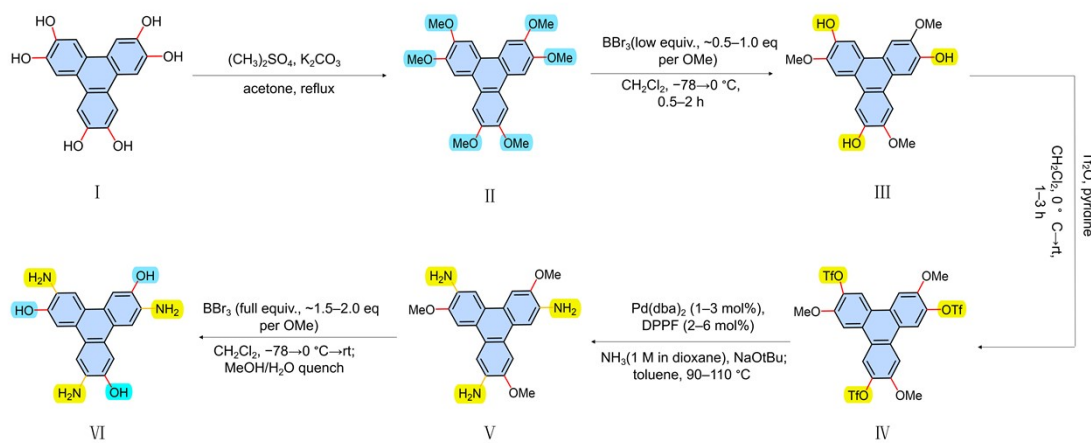


**Fig. S3.** Synthetic route to TTTP showing methylation, partial demethylation, triflation and Pd-catalysed amination steps.

## Computational details for Poisson's ratio and The Young's modulus

Angle-dependent mechanical properties, including Young's modulus and Poisson's ratio, were computed using established analytical formulae derived from the elastic tensor to evaluate the anisotropic mechanical behaviour of the material.

$$E(\theta) = \frac{C_{11}C_{22} - C_{12}^2}{C_{11}\sin^4\theta + C_{22}\cos^4\theta + (\frac{C_{11}C_{22} - C_{12}^2}{C_{44}} - 2C_{12})\cos^2\theta\sin^2\theta}$$

$$\nu(\theta) = \frac{\left(C_{11} + C_{22} - \frac{C_{11}C_{22} - C_{12}^2}{C_{44}}\right)\cos^2\theta\sin2\theta - C_{12}(\cos^4\theta + \sin^4\theta)}{C_{11}\sin^4\theta + C_{22}\cos^4\theta + (\frac{C_{11}C_{22} - C_{12}^2}{C_{44}} - 2C_{12})\cos^2\theta\sin^2\theta}$$

## Comparison of band structure calculated in vacuum and aqueous solution

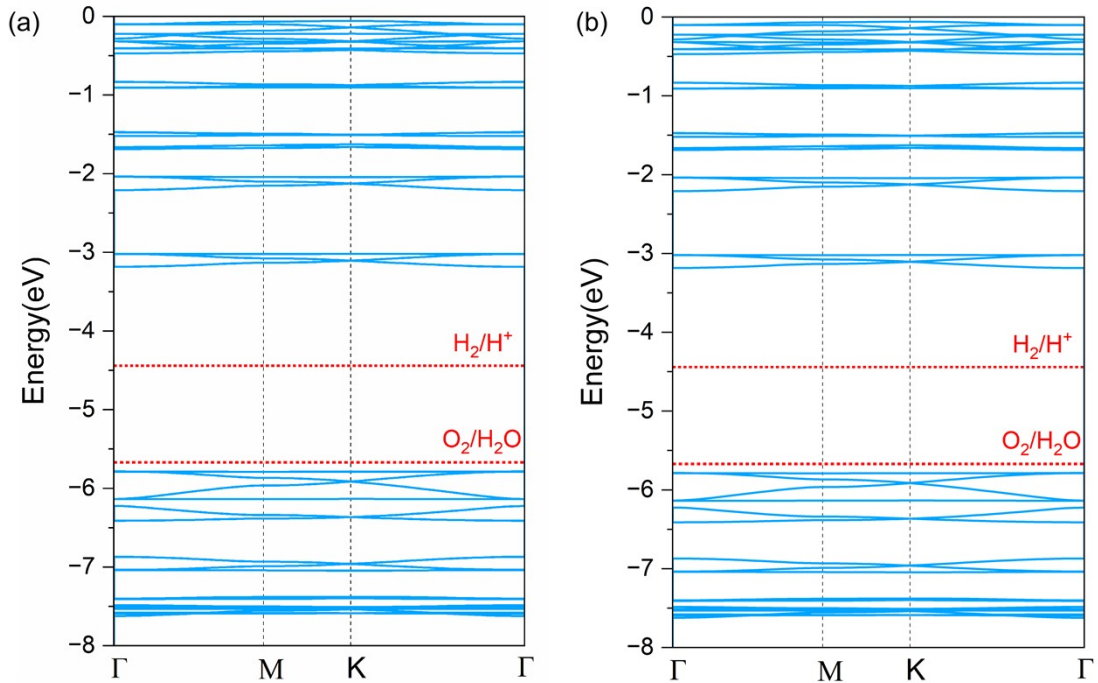


**Fig. S4** (a) Calculated band structure in vacuum. (b) Calculated band structure in aqueous solution; red dashed lines mark the redox potentials of  $\text{H}^+/\text{H}_2$  and  $\text{O}_2/\text{H}_2\text{O}$ .

Table. S1 Calculated bandgap, VBM and CBM energy levels of 2D CTF in vacuum and in aqueous solution in SHE06 level.

2D CTF	Bandgap (eV)	VBM (eV)	CBM (eV)
Vacuum	2.61	-5.79	-3.18
Implicit solvent	2.63	-5.76	-3.13

### Calculated $\eta_{STH}$ as a function of QE for 2D CTF and various COFs

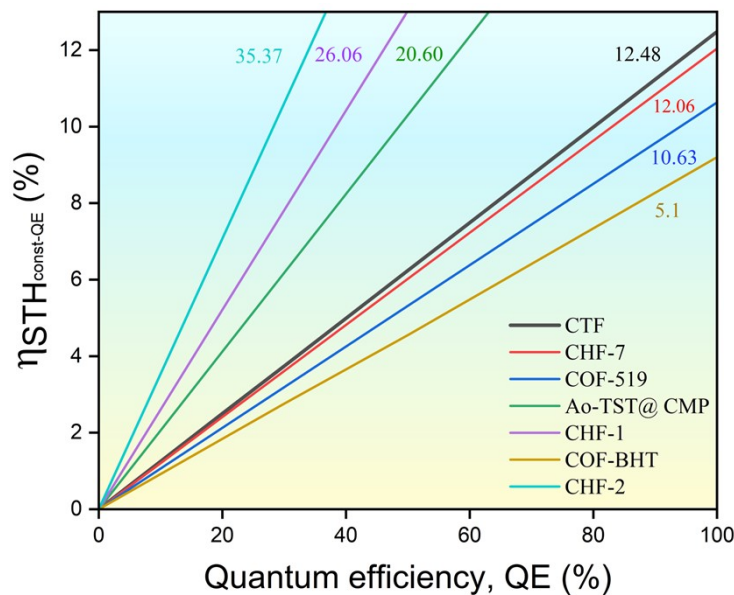


**Fig. S5** Calculated solar-to-hydrogen (STH) efficiency as a function of quantum efficiency (QE) for CTF and various COFs photocatalysts under identical absorption conditions.

## Adsorption of H<sub>2</sub>O molecules on the surfaces of 2D CTF

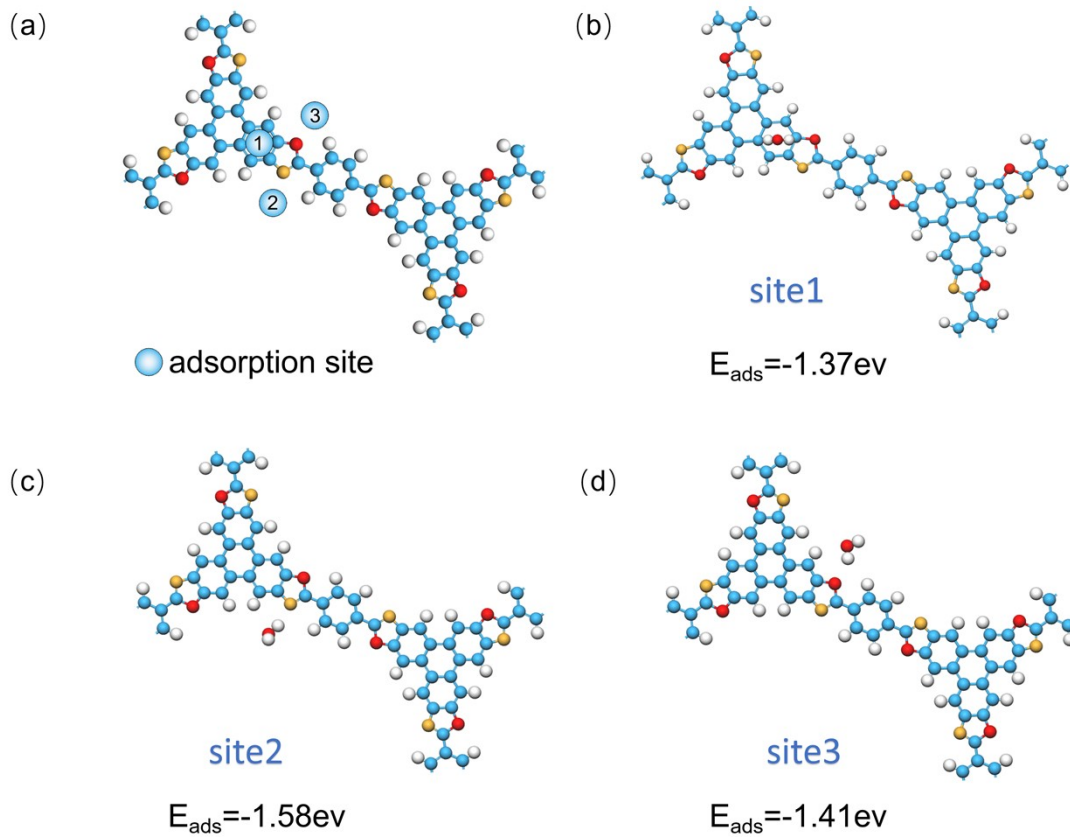


**Fig. S6.** (a-c) Water adsorption geometries at site1, site2, and site3, respectively. The corresponding adsorption energies ( $E_{ads}$ ) are  $-1.37\text{ eV}$ ,  $-1.58\text{ eV}$ , and  $-1.41\text{ eV}$ . (d) The unit cell of CTF

To identify the most favourable adsorption sites for water activation on the CTF framework, we calculated the adsorption free energies (approximated by adsorption energies,  $E_{ads}$ ) of H<sub>2</sub>O at three different surface sites, as illustrated in Figure S3.

The adsorption energy was calculated using the following formula:

$$E_{abs} = E_{H_2O/slab} - E_{slab} - E_{H_2O}$$

where  $E_{H_2O/slab}$  is the total energy of the system after adsorption,  $E_{slab}$  is the total energy of the pristine material, and  $E_{H_2O}$  is the energy of an isolated water molecule in the gas phase.

The adsorption process was simulated by placing a single water molecule onto each representative site (site1, site2, and site3), followed by structural optimization.

The corresponding adsorption energies were determined as  $E_{ads}(\text{site1}) = -1.37$  eV,  $E_{ads}(\text{site2}) = -1.58$  eV, and  $E_{ads}(\text{site3}) = -1.41$  eV. Among them, site2 exhibits the most negative adsorption energy, indicating a stronger interaction between the water molecule and the framework at this position. This suggests that site2 may serve as a preferential location for water activation and subsequent catalytic steps, such as O–H bond cleavage and the initiation of the OER. The variation in  $E_{ads}$  among the three sites highlights the spatially heterogeneous catalytic nature of the CTF surface.

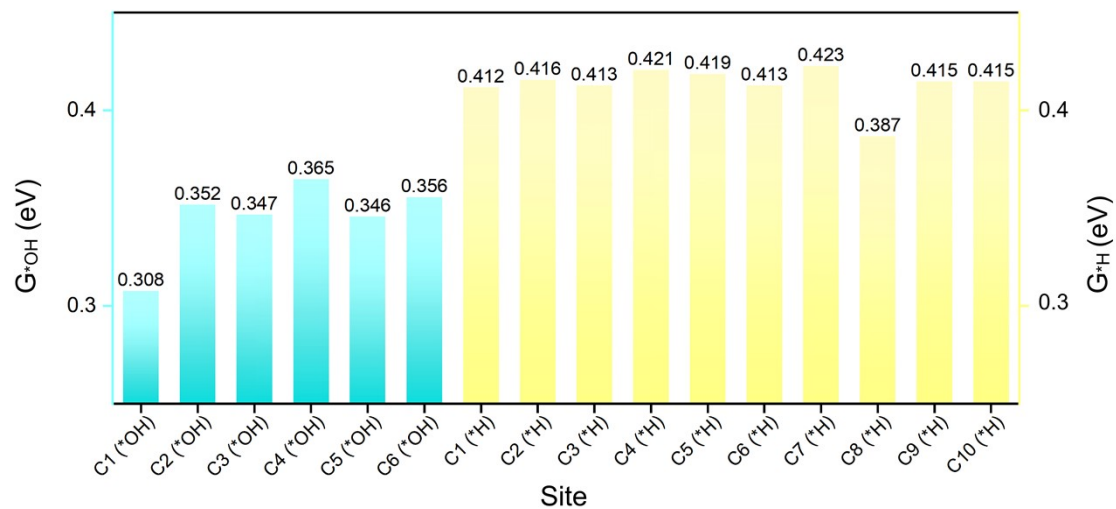


**Fig.S7** The calculated  $\Delta G^*_{OH}$  on the C atoms contributing to VB and  $\Delta G^*_{H}$  on C1-C10 atoms.

## COHP/ICOHP analysis of key adsorbate-substrate bonds

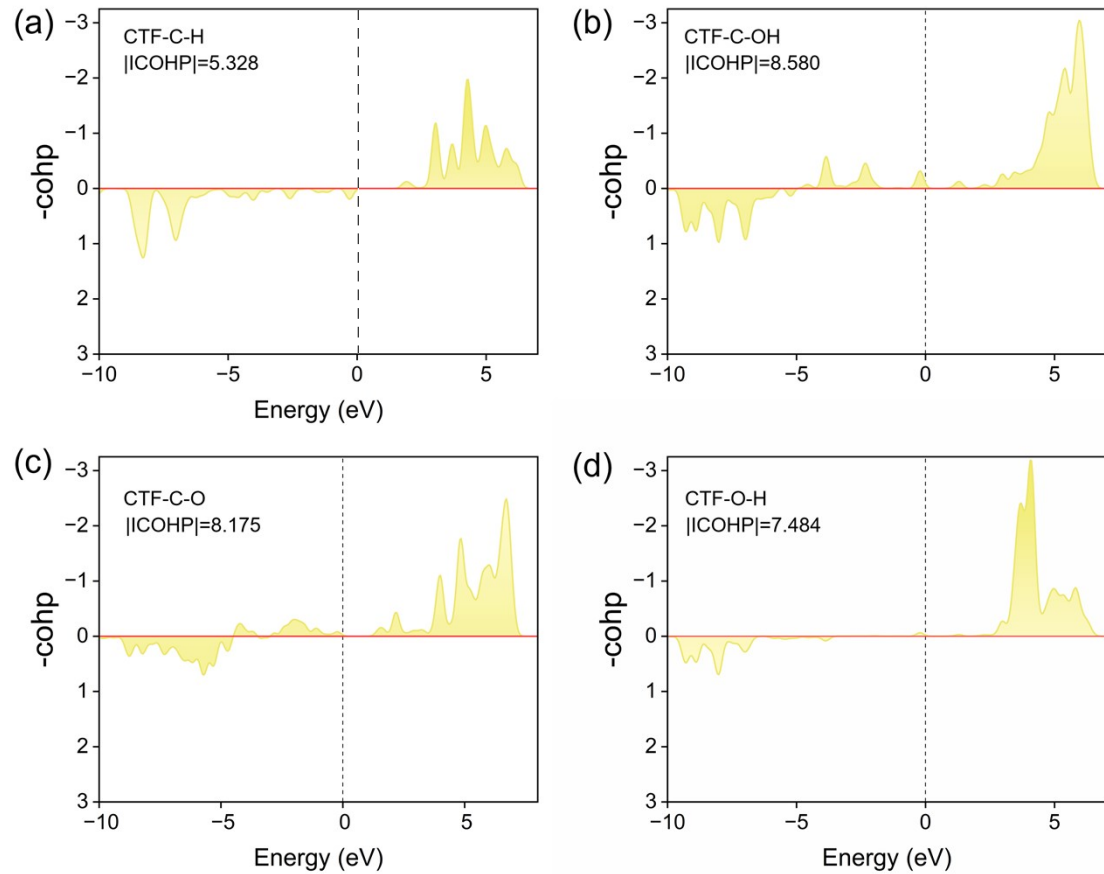


**Fig.S8** (a) -COHP of C-H (HER) on 2D CTF; EF=0 (dashed).  $|\text{ICOHP}|=5.328 \text{ eV}\cdot\text{bond}^{-1}$ . (b) -COHP of C-O (OH\*) on 2D CTF; EF=0 (dashed).  $|\text{ICOHP}|=8.580 \text{ eV}\cdot\text{bond}^{-1}$ . (c) -COHP of C-O (O\*) on 2D CTF; EF=0 (dashed).  $|\text{ICOHP}|=8.175 \text{ eV}\cdot\text{bond}^{-1}$ . (d) -COHP of O-H (OH\*) on 2D CTF; EF=0 (dashed).  $|\text{ICOHP}|=7.484 \text{ eV}\cdot\text{bond}^{-1}$ .

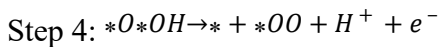
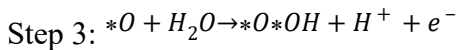
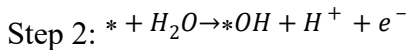
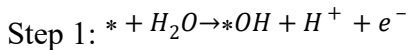
## Computational details for carrier mobility

Table. S2 Calculated  $m^*/m_d$ ,  $C_{2d}$ ,  $E_{2d}$  and  $\mu$  of 2D CTF along x and y directions.

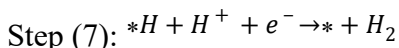
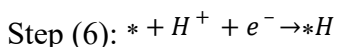
	Carrier	$m^*/m_e$	$m_d$	$C_{2d}$ (J/m <sub>2</sub> )	$E_{2d}$	$\mu$ (cm <sub>2</sub> /V·s)
x	e <sup>-</sup>	0.52	0.49	31.33	1.33	$3.06 \times 10^3$
y	e <sup>-</sup>	0.46	0.49	31.33	3.34	$4.64 \times 10^2$
x	h <sup>+</sup>	0.91	1.03	30.48	1.25	$9.04 \times 10^2$
y	h <sup>+</sup>	1.16	1.03	30.48	3.15	$1.41 \times 10^2$

## Computational details for free energy change and formation energy

In aqueous solution, OER process could be decomposed into four one-electron oxidation steps, corresponding to the deprotonation of water molecules, as follows<sup>1</sup>:



Meanwhile, HER process could be decomposed into two one-electron steps with each step consuming a proton and an electron:



Where \* denotes a site on the surface, \*(radical) denotes the corresponding radical adsorbed on the surface. In particular, the third step in OER process. To calculate the free energy changes involved in OER and HER process, Gibbs free energies:  $G(T) = E + H(T) - TS(T)$  with  $E$  denoting the self-consistent field energy for a given species, can be calculated including all relevant finite temperature contributions to enthalpy  $H(T)$  and entropy  $S(T)$ , i.e. vibration, rotation and translation for gas phase species; for adsorbed species only vibrational contributions were considered since rotational and translational motions become frustrated. To quantitatively assess the

thermodynamics of each elementary step in the OER and HER pathways on the 2D CTF surface, the corresponding Gibbs free energy changes ( $\Delta G$ ) were computed by taking into account the effects of solvent pH and the external electrochemical potential ( $U$ ). Under standard conditions ( $\text{pH} = 0$ ,  $T = 298$  K, 1 atm), the electrochemical potential of the proton-electron pair ( $\text{H}^+ + \text{e}^-$ ) is approximated by  $\frac{1}{2}G(\text{H}_2)$ , reflecting the equilibrium in the half-reaction  $\text{H}^+ + \text{e}^- \rightleftharpoons \frac{1}{2}\text{H}_2$ .

The pH dependence was incorporated using the Nernstian correction term  $\Delta \text{pH} = 0.059 \times \text{pH}$  (in eV), and the influence of photoexcited charge carriers was modeled by applying an external potential correction term ( $eU$ ), where  $U_e$  and  $U_h$  correspond to the oxidation and reduction potentials for OER and HER, respectively. These are derived from the energetic offset between the valence band maximum (VBM) or conduction band minimum (CBM) and the Computational Hydrogen Electrode (CHE) level.

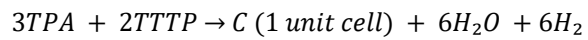
The expressions for the Gibbs free energy changes of each step are given as:

$$\begin{aligned}\Delta G_i &= G(*H) - G(*) - \frac{1}{2}G(\text{H}_2) + \Delta \text{pH} - eU_e \\ \Delta G_{ii} &= G(*) - G(*H) + \frac{1}{2}G(\text{H}_2) + \Delta \text{pH} - eU_e \\ \Delta G_1 &= \frac{1}{2}G(\text{H}_2) + G(*\text{OH}) - G(*) - G(\text{H}_2\text{O}) - \Delta \text{pH} - eU_h \\ \Delta G_2 &= \frac{1}{2}G(\text{H}_2) + G(*\text{O}) - G(*\text{OH}) - \Delta \text{pH} - eU_h \\ \Delta G_3 &= \frac{1}{2}G(\text{H}_2) + G(*\text{O*OH}) - G(*\text{O}) - G(\text{H}_2\text{O}) - \Delta \text{pH} - eU_h \\ \Delta G_4 &= \frac{1}{2}G(\text{H}_2) + G(*\text{OO}) - G(*\text{O*OH}) - \Delta \text{pH} - eU_h \\ \Delta G_5 &= G(*) + G(\text{O}_2) - G(*\text{OO})\end{aligned}$$

These calculations allow for a comprehensive energetic analysis of both half-reactions in the context of photocatalytic overall water splitting, providing insight into the thermodynamic feasibility and rate-determining steps under various operating conditions.

To assess the thermodynamic feasibility of CTF framework formation, we calculated the average reaction energy ( $E_r$ ) based on a representative condensation reaction between terephthalaldehyde (TPA) and 13,15,17-trihydroxy-14,16,18-triaminotriphenylene (TTTP), as illustrated in Figure 1. The reaction proceeds via a

dehydration and hydrogen release process:



The formation energy is calculated as:

$$E_f = E(CTF) + 6E(H_2O) + 6E(H_2) - 3E(TPA) - 2E(TTTP)$$

Here, E refers to the DFT-calculated total energy of each molecular or framework species.

## References

- 1 A. A. Peterson, F. Abild-Pedersen, F. Studt, J. Rossmeisl and J. K. Nørskov, *Energy Environ. Sci.*, 2010, **3**, 1311.
- 2 K. Mathew, R. Sundararaman, K. Letchworth-Weaver, T. A. Arias and R. G. Hennig, *J. Chem. Phys.*, 2014, **140**, 084106.
- 3 J. Qiao, X. Kong, Z.-X. Hu, F. Yang and W. Ji, *Nat. Commun.*, 2014, **5**, 4475.
- 4 S. Maintz, V. L. Deringer, A. L. Tchougréeff and R. Dronskowski, *J. Comput. Chem.*, 2016, **37**, 1030–1035.
- 5 M. Wang, X. Zhang, Y. Chen and D. Li, *J. Phys. Chem. C*, 2016, **120**, 5059–5066.
- 6 A. A. Peterson, F. Abild-Pedersen, F. Studt, J. Rossmeisl and J. K. Nørskov, *Energy Environ. Sci.*, 2010, **3**, 1311.
- 7 R. Shen, C. Qin, L. Hao, X. Li, P. Zhang and X. Li, *Adv. Mater.*, 2023, **35**, 2305397.